

Green Synthesis of Manganese Dioxide Nanoparticles and its Biological

Sabeeha K. Shanshool *, Zainab J. Shanani 

Department of Physics, College of science for Women, University of Baghdad, Baghdad, Iraq.

*Corresponding Author.

Received 19/01/2023, Revised 06/05/2023, Accepted 08/05/2023, Published Online First 20/10/2023,
Published 01/05/2024



© 2022 The Author(s). Published by College of Science for Women, University of Baghdad.

This is an Open Access article distributed under the terms of the [Creative Commons Attribution 4.0 International License](https://creativecommons.org/licenses/by/4.0/), which permits unrestricted use, distribution, and reproduction in any medium, provided the original work is properly cited.

Abstract

The goal of this research is to prepare Manganese dioxide (MnO_2) nanoparticles from plant extracts (*Punica granatum L peel*, *Artemisia herba-alba Asso*, *Matricaria chamomilla L*, and *Camellia sinensis*) and test their antibacterial activity. To evaluate the presence of phytochemicals in plant extracts, were used UV-Visible spectrophotometer analysis (UV– Vis), Zeta potential (ZP), and X-ray Diffraction (XRD). The production of MnO_2 nanoparticles by plant extracts was shown to have distinctive features. The average crystallite size of manufactured MnO_2 NPs was calculated to be between 14.22-21.0 nm, with zeta potential values -23.6, -20.04, -25.6, -16.7 mV, respectively. Manganese dioxide nanoparticles (MnO_2 NPs) have significant antibacterial activity against fungi and diverse gram-positive and gram-negative bacteria. The findings results showed that the synthesized MnO_2 NPs by *P granatum L peel*, *A herba-alba Asso*. plants had the highest percentage of bacterial and fungi inhibition, while *M. chamomilla L*. and *C. sinensis* extracts showed lower antifungal activity

Keywords: Antimicrobial, Fungi, Manganese dioxide (MnO_2), *P granatum L peel*, Zeta potential (ZP).

Introduction

Nanoparticles are microscopic things that act in terms of transport and properties as if they were a single entity. Examples include liposomes, Nanocrystals, Nano suspension, Solid lipid nanoparticles (SLN), and other nanoparticles. As a new generation of ecologically benign catalysts, nano- MnO_2 has a lot of potential in the field of environmental protection. A lot of investigations have discovered that the structure of semiconductor materials influences their functional activity.¹ Manganese dioxide is one of the most intriguing materials since it has a diverse structure and large surface area. Manganese dioxides' diverse structural and chemical properties are used to benefit possible applications such as cation-exchange, ion and molecular separation; absorbents, sensors, batteries,

and catalysis.² Microorganisms capable of generating nanoparticles include bacteria, fungi, and algae. The principle is the reduction of metal ions to nanoparticles.³ Manganese dioxide NPs have got a lot of attention because of their wide range of applications in sectors like catalysis, chemical sensing devices, ion-sieves, microelectronics,⁴ rechargeable batteries, and optoelectronics.⁵ They are also based on earth's extra elements due to the presence of many attachments for a variety of activities. Mn is the twelfth most prevalent element on the planet and the third most common transition element after Fe and Ti.⁶ For dye degradation, MnO_2 NPs show a strong photocatalytic activity.^{7,8} Although physical and chemical methods can be used to synthesize nanoscale materials, green

manufacturing is the best alternative because it is more environmentally friendly.^{9,10} Plant extracts can be used to create nanoscales instead of conventional biological techniques such as the microbial approach, which includes the time-consuming process of maintaining cell cultures.^{11,12} MnO₂ NPs were used to test antibacterial activity against four strains of bacteria (*B. Subtilis*, *S. aureus*, *E. coli*. and *K. pneumonia*) and one yeast (*C. albicans*). The

aim of the research is to prepare the oxide in an environmentally friendly and inexpensive way, use of several plants in the preparation of manganese oxide nanoparticles Like (*P granatum L peel* A *herba-alba.Asso* and *M chamomilla L*, *C sinensis*), study the physical properties of the prepared material and measure the biological activity of the prepared material on several types of bacteria and fungi.

Materials and Methods

Green methods of synthesis Manganese dioxide nanoparticles

Collecting of plant material:

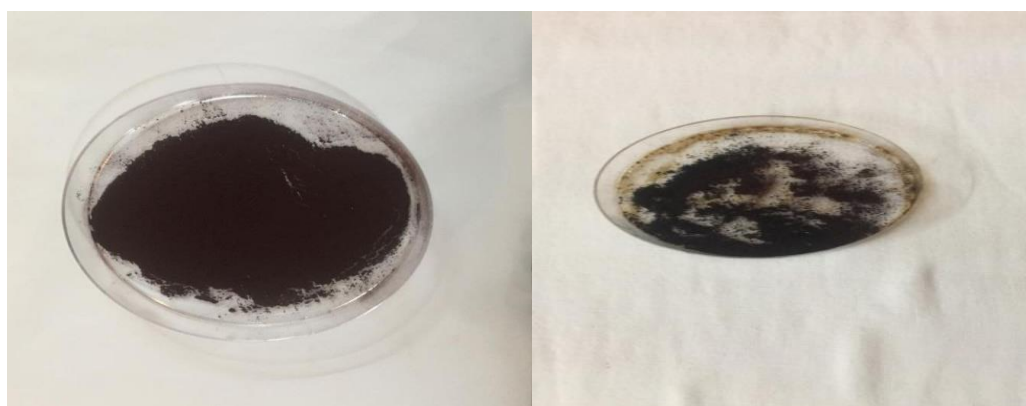
A herba-alba Asso. *M chamomilla L*, *P granatum L peel* and *C sinensis* were collected from the local market in Baghdad, the plants were kept at room temperature until use.

The preparation of hot aqueous extract of *P granatum L peel*, *A herba-alba Asso*, *M chamomilla L*, and *C sinensis*.

The leaf powder (10gm) was mixed well with 150 ml distilled water boiled at 80°C, and then homogenized on a magnetic stirrer for 2 hours, although the color of the aqueous solution was different. The aqueous solution was then filtered and centrifuged for 20 minutes at 6000 rpm before being stored at 4°C until being used.

The synthesis of MnO₂ NPs by using aqueous extract of *P granatum L peel*, *A herba-alba Asso*, *M chamomilla L*. and *C sinensis*.

The initial solution was made by, 0.2 g of manganese acetate(CH₃COOH)₂Mn.6H₂O was mixed with 100 ml of distilled water and heated for ten minutes with magnetic stirring. To prepare MnO₂ nanoparticles, 50 ml of the manganese acetate solution was mixed with 5 ml aqueous extracts from *P granatum L peel*, *A herba-alba Asso*, *M chamomilla L* and *C sinensis* extracts on a magnetic stirrer at 70°C for 60 minutes, despite the fact that the color of the aqueous solution varies. The hue of the solution changed to brown when manganese acetate was added to both *P granatum L peel*, *M chamomilla L* and *C sinensis* extracts, The hue of the solution changed to dark brown when it was mixed with extracts of *A. herba- alba.Asso*. The sample was then centrifuged at 8000 rpm for 15 minutes. The solution was baked at 250°C for 2 hours, and the powder was carefully collected and kept for future use see Fig 1.



(a)

(b)

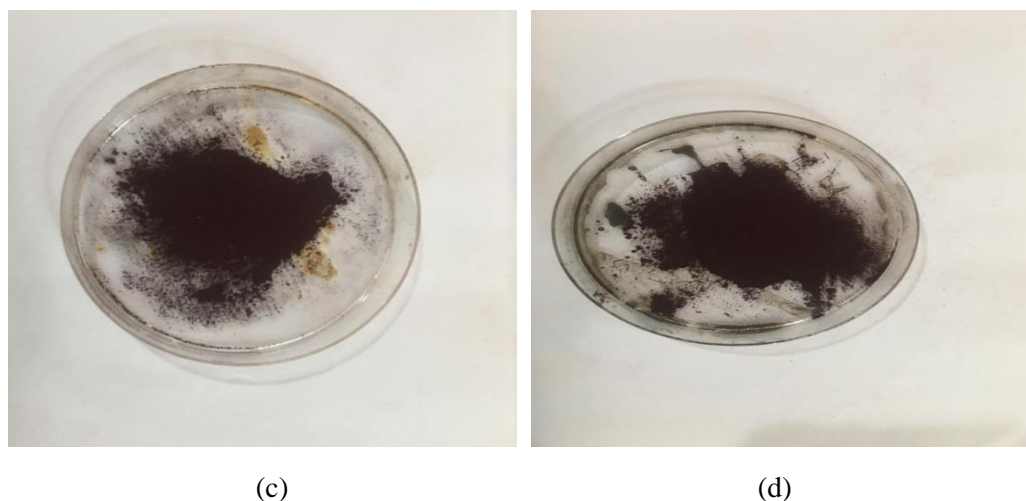


Figure1. Manganese dioxide nanoparticles green synthesized via (a) *P granatum L peel*, (b) *A herba-alba Asso* extract, (c) *M chamomilla L* extract, (d) *C sinensis* extract.

Biological efficacy method

The antibacterial activity of manganese dioxide nanoparticles on Mueller-Hinton agar (MHA) was examined using the good diffusion method (Merck). Inhibition zones against gram negative bacteria (*E. coli*, *K. pneumonia*), gram positive bacteria (*S aureus*, *B Subtilus*), and fungal isolates (*C albicans*) were measured in millimeters (well size was 6 mm).^{13,14} MHA agar plates were infected with bacterial strains under aseptic circumstances, and wells were filled with 50 MnO₂ NPs at several concentrations (100, 75, 50, 25%) and incubated at 37°C for 24

hours. The inhibition zones were measured after the incubation period.¹⁵

Characterization

UV-visible spectrometer (UV amersham bioscience libra s32 england), Powder XRD (XRD Siemens model D500) and Zeta potential (Dls zeta Malvern Zetasizer nanozs) were used to characterize the produced MnO₂ nanoparticles in order to explore their structural and optical properties.

Results and Discussion

UV – visible spectrum Studies

The UV-visible of green MnO₂ NPs was used to assess band gap and the absorption maxima of biological molecules involved in the reduction and capping from *P granatum L peel*, *A herba-alba Asso*, *M chamomilla L*, and *C sinensis* extracts. as shown in Table 1. The UV-visible study revealed

that plant extracts have absorption maxima in the UV region 310–390 nm as shown in Fig 2, The energy gap is determined by Eq 1¹⁶:

$$E_g = hv / \lambda \dots\dots 1$$

Where E_g : Energy gap, λ : wavelength, hv : Photon energy.+

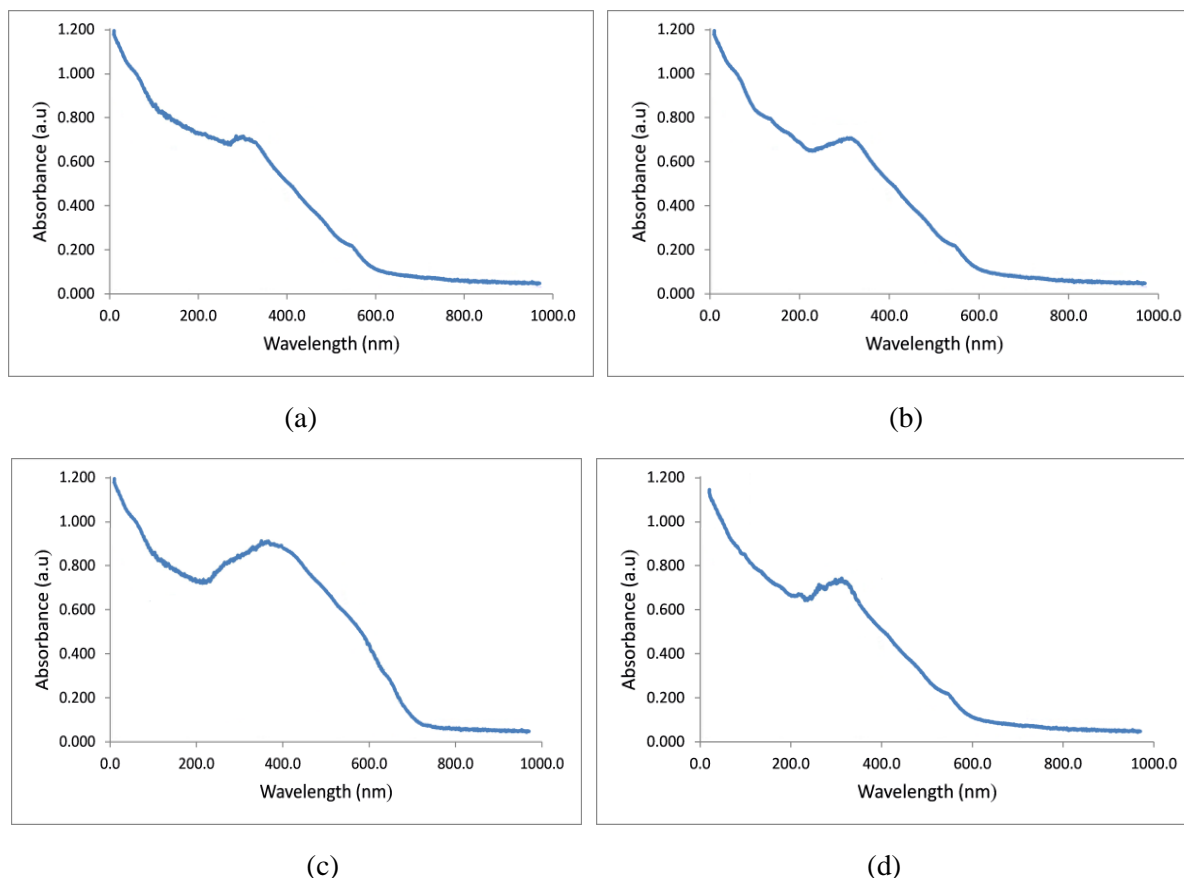


Figure 2. UV-visible of green-synthesized of MnO₂ NPs using, (a) *P granatum L peel* extract, (b) *A herba-alba Asso* extract, (c) *M chamomilla L* extract, (d) *C sinensis* extract.

Table 1. Band gaps from UV-Vib absorption spectra of the MnO₂.

MnO ₂ NPs isolates	Absorption Wavelength (nm)	Band gap (mV)
<i>P granatum L peel</i>	300	4.13
<i>A herba-alba Asso</i>	320	3.87
<i>M chamomilla L</i>	380	3.26
<i>C sinensis</i>	305	4.06

Powder XRD Studies

The manganese dioxide nanoparticles' crystalline size and nature were confirmed by X-ray diffraction analysis. Fig 3a, b shows an XRD pattern of green-synthesized MnO₂ NPs via *P granatum L peel*, *A herba-alba Asso*. XRD pattern demonstrates distinguish peaks at $2\theta=28.51^\circ$, 30.51° , 35.20° ,

43.17° , 50.72° , 56.41° , 68.32° and 75.71° indexed to (310), (101),(222),(301), (411),(110),(002) and (217) crystal plane of MnO₂ NPs (JSPDF 44-0141).^{17,18} The obtained results are in good agreement with the JCPDS pdf number of 10799;¹⁹ In addition, the XRD pattern shows that MnO₂ NPs are extremely crystalline, which is demonstrated by the intensity of the peaks and supported by a comparison of the acquired XRD spectrum with the reference material. Eq 2 the Debye Scherrer condition is used to calculate the crystallite measure²⁰.

$$D = 0.9\lambda/\beta\cos\theta\dots 2$$

Where λ is the X-beam wave length, β is the line expanding at a large portion of the greatest power in radians, θ is the Bragg point. The average particle size was discovered to be 14.22 and 18.61 nm, respectively. The XRD pattern of green-synthesized MnO₂ NPs by *M. chamomilla L.* and *C. sinensis*

was shown in Fig 3c,d. The XRD pattern results showed that various diffraction peaks, which agree with JCPDS no. 78-0424 as indexing to (101), (301), (210), (411), (116), (220) and (300) crystal planes at crystal planes 30.28, 43.70, 44.67, 50.67, 56.27, 64.73 and 72.35 degrees, respectively. The Miller index (101) and (301) had the highest peak intensity at a 30.28 and 43.70-degree angles. The

enhanced peak intensity and crispness of the synthesized NPs further confirmed that they are extremely crystalline.²¹ The average particle size was discovered to be 21.0 and 16.07 nm, respectively, as shown Table 1. The inexplicable reflections could be caused by the crystallization of bio-organic molecules on the surface of nanoparticles.²²

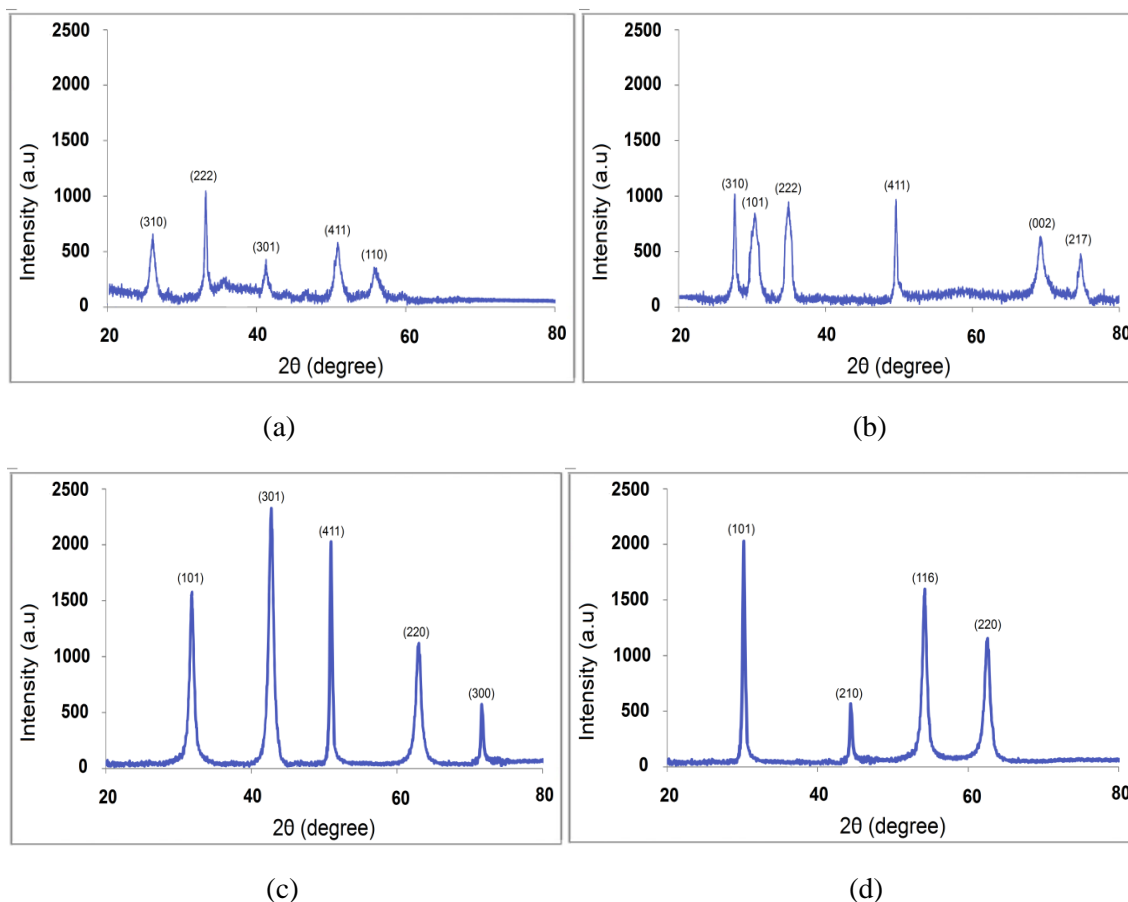


Figure 3. X-ray diffraction (XRD) pattern of MnO₂ NPs synthesized via (a) *P granatum L peel* extract, (b) *A herba-alba Asso* extract, (c) *M chamomilla L* extract, (d) *C sinensis* extract.

Table 2. Crystalline size of MnO₂ NPs.

MnO ₂ NPs isolates	Average grain size (nm)
<i>P granatum L peel</i>	14.22
<i>A herba-alba Asso.</i>	18.61
<i>M chamomilla L</i>	21.0
<i>C sinensis</i>	16.07

Zeta potential analysis

The stability of colloidal nanoparticles is demonstrated by ZP. at 500 mJ laser power and 500

pulses, the zeta potential values of green-synthesized MnO₂ NPs utilizing *P granatum L peel*, *A herba-alba Asso*, *M chamomilla L*, and *C sinensis* extracts were -23.6, -20.04, -25.6, and -16.7mV, respectively²³. More negative values in the colloidal solution suggest that the NPs are more stable,²⁴ as shown in Fig. 4.

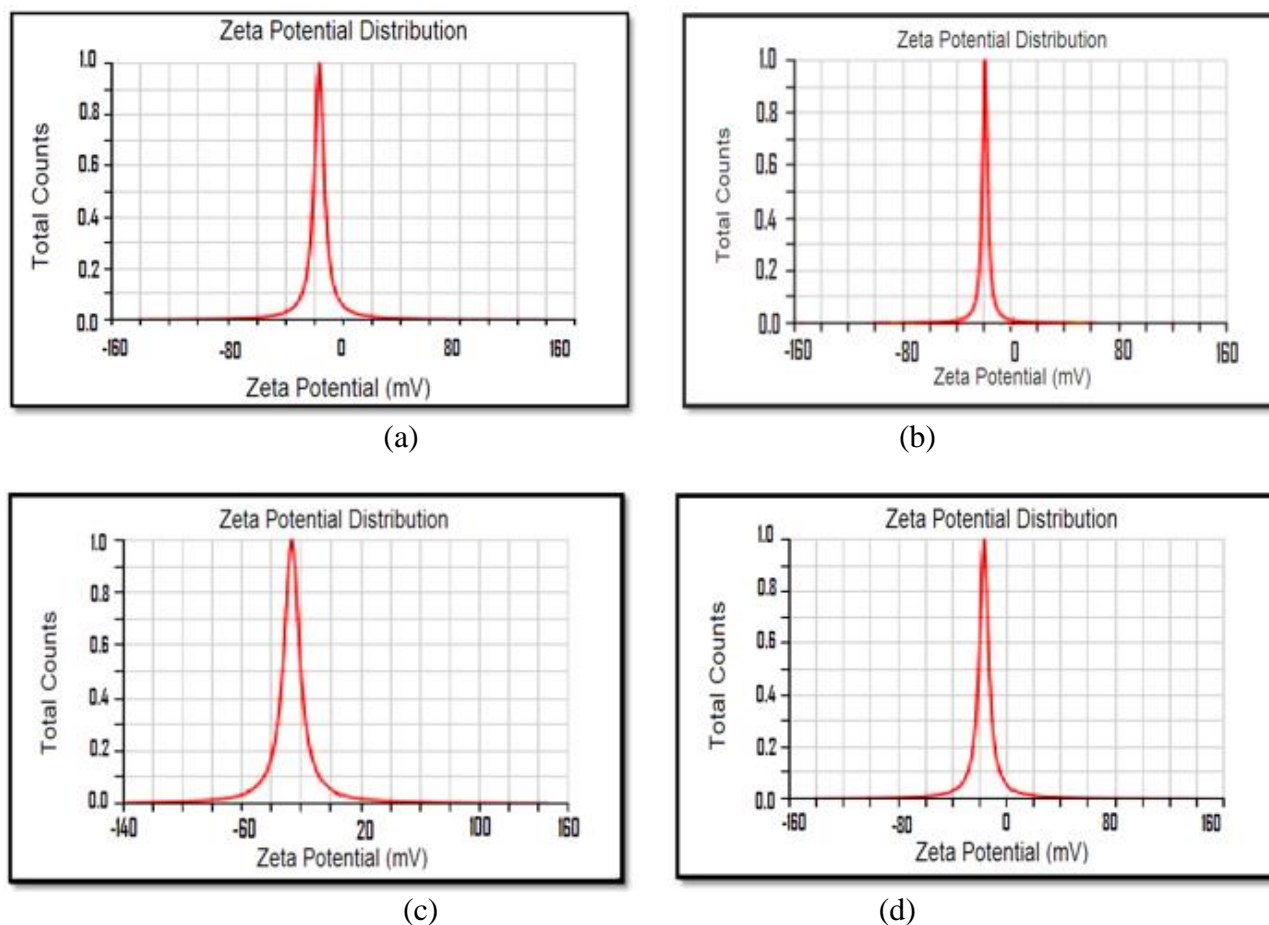


Figure 4. Zeta potential analysis of green-synthesized of MnO₂ NPs using (a) *P granatum L peel* extract (b) *A herba-alba Asso* extract (c) *M chamomilla L* extract (d) *C sinensis* extract

Antimicrobial activity

The results also showed that the producer of green synthesized MnO₂ NPs via *P granatum L peel*, *A herba-alba Asso*, *M chamomilla L* and *C sinensis* extracts, were more active toward Gram-negative species (*E. coli*, *K. pneumonia*) than Gram-positive species (*S aureus*, *B Subtilus*) Manjula *et al*, were also reported the same inhibitory effect of MnO₂ NPs toward Gram-positive than Gram-negative bacteria²⁵. This could be due to structural and compositional differences in the cell walls of Gram-negative and Gram-positive bacteria^{26,27}, and as shown in Fig 5. According to several studies, the majority of nanoparticles antibacterial activity is caused by physical and chemical degradation, such as the dissolution of lipid molecules and oxidative stress.²⁸ A synergistic interaction between the physical characteristics of the nanoparticle and the adsorption of biologically active phytomolecules from the *P granatum L peel*, *A herba-alba Asso*, *M*

chamomilla L, and *C sinensis* extracts on their surface and other plant materials may also contribute to the enhanced antibacterial action of MnO₂ NPs²⁹⁻³¹. To demonstrate the findings the results showed that the synthesized MnO₂ NPs significantly reduced the killing efficiency of MnO₂ NPs using *P. granatum.L peel* and *A herba-alba Asso*. extracts of *C albicans*, as shown in Fig 6. MnO₂ NPs by *M. chamomilla L*. and *C sinensis* extracts showed lower antifungal activity than MnO₂ NPs by *P granatum L peel* and *A herba-alba Asso*. extracts, as shown in Table 3. This shows that physiologically active phytomolecules, particularly efficient at killing fungal strains, are present in the *P granatum L peel* and *A herba-alba Asso*. extract.³²

The numbers 9, 10, 11 and 12 refer to Manganese dioxide nanoparticles prepared by the extracts (*P granatum L peel*, *A herba-alba Asso*, *M. chamomilla L* and *C sinensis*) respectively.

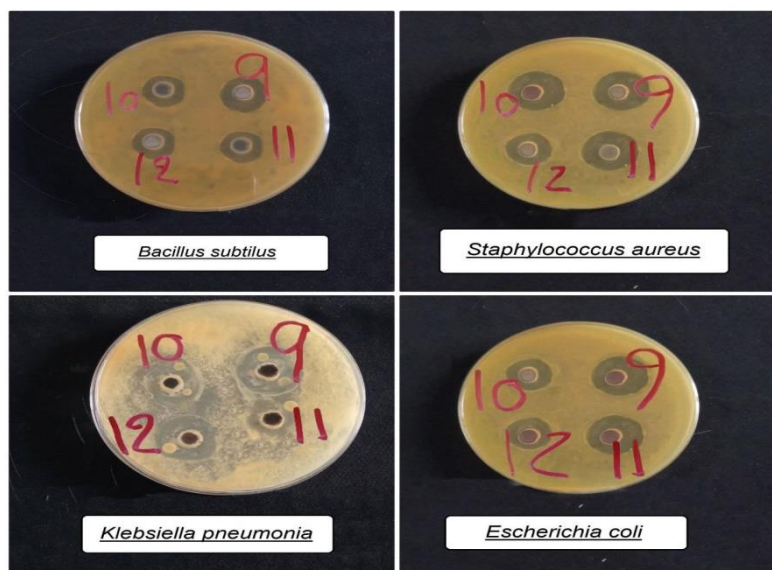


Figure 5. Representative images of control and treated for gram-positive and gram-negative bacteria

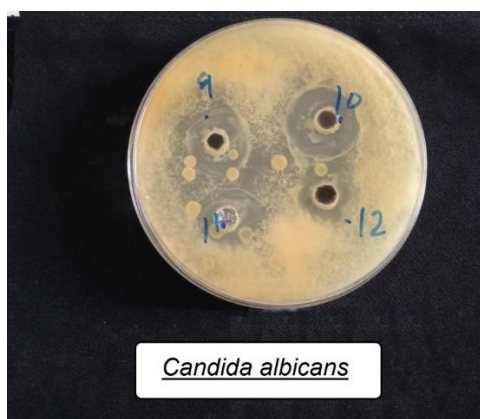


Figure 6. Representative images of control and treated for fungi (*C albicans*)

Table 3. Measurement of inhibition diameters of MnO₂ nanoparticles on bacteria and fungi

Samples	Zone of inhibition (mm)				
	<i>S aureus</i>	<i>B Subtilus</i>	<i>E coli</i>	<i>K pneumonia</i>	<i>C albicans</i>
9	23	15	16	25	26
10	23	17	24	24	25
11	15	16	23	23	23
12	20	15	17	16	17

Conclusion

In this research, we focused on the various plant species' capacity to green synthesis NPs. Over conventional physical and chemical methods, plant-mediated NP synthesis offers undeniably considerable advantages. Using a green synthesis method, MnO₂ nanoparticles were produced from the peels of *P granatum L*, *A herba-alba Asso*, *M*

chamomilla L, and *C sinensis*. The creation of pure and crystalline MnO₂ nanoparticles was validated by XRD and UV-visible. Based on the results of the XRD, we deduced that the generated manganese dioxide nanoparticles were extremely crystalline in nature. The manganese dioxide nanoparticles ranged in size from 14.22 to 21.0 nm on average

and they showed significant antibacterial action. The research results demonstrate Manganese dioxide nanoparticles from the green technique can inhibit the growth of *E coli*, *K pneumonia*, *S aureus*,

B subtilus, and *C albicans*, where we conclude from the above results that manganese dioxide prepared by *A herba-alba* Asso the extract has the highest percentage of inhibition of bacteria and fungi.

Acknowledgment

The cooperation of the Nano Lab, Department of Physics, College of Science for Women, University of Baghdad appreciated.

Authors' Declaration

- Conflicts of Interest: None.
- We hereby confirm that all the Figures and Tables in the manuscript are ours. Furthermore, any Figures and images, that are not ours, have been included with the necessary permission for

- re-publication, which is attached to the manuscript.
- Ethical Clearance: The project was approved by the local ethical committee in University of Baghdad.

Authors' Contribution Statement

Z. J. Sh. proposed the topic of research and guidance and the review and proofreading the research. S. K. Sh. prepared the samples and

analyzed parameters and writing, as well as the costs and publishing process.

References

1. Burda C, Chen X, Narayanan R, El-Sayed MA. Chemistry and Properties of Nanocrystals of Different Shapes. *Chem Rev.* 2005; 105(4): 1025–1102. <https://dx.doi.org/10.1021/cr030063a>.
2. Narayanan KB, Sakthivel N. Biological synthesis of metal nanoparticles by Microbes. *Adv Colloid Interface Sci* 2010; 156(2): 1-13. <https://dx.doi.org/10.1016/j.cis.2010.02.001>.
3. Thakkar KN, Mhatre SS, Parikh RY. Biological synthesis of metallic Nanoparticles. *Nanomed Nanotechnol Biol Med.* 2010; 6(2): 257-262. <https://dx.doi.org/10.1016/j.nano.2009.07.002>.
4. Abidi SH, Sherwani SK, Siddiqui TR, Bashir A, Kazmi SU. Drug resistance profile and biofilm forming potential of *Pseudomonas aeruginosa* isolated from contact lenses in Karachi-Pakistan. *BMC Ophthalmol.* 2013; 13(57): 1471-2415. <https://dx.doi.org/10.1186/1471-2415-13-57>.
5. Han C, Romero N, Fischer S, Dookran J, Berger A, Doiron AL. Recent developments in the use of nanoparticles for treatment of biofilms. *Nanotechnol Rev.* 2017; 6(5): 383–404. <https://dx.doi.org/10.1515/ntrev-2016-0054>.
6. Lu Y, Cai W-j, Ren Z, Han P. The Role of Staphylococcal Biofilm on the Surface of Implants in Orthopedic Infection. *Microorganisms.* 2022; 10(10): 1909. <https://doi.org/10.3390/microorganisms10101909>.
7. Bhattacharyya P, Agarwal B, Goswami M, Maiti D, Baruah S, Tribedi P. Zinc oxide nanoparticle inhibits the biofilm formation of *Streptococcus pneumoniae*. *Anton Leeuw.* 2018; 111(1): 89–99. <https://dx.doi.org/10.1007/s10482-017-0930-7>.
8. Kilty JS, Desrosiers YM. The role of bacterial biofilms and the pathophysiology of chronic rhinosinusitis. *Curr Allergy Asthma Rep.* 2008; 8(3): 227–233. <https://dx.doi.org/10.1007/s11882-008-0038-2>.
9. Taylor EN, Kummer, KM, Durmus NG, Leuba K, Tarquinio KM, Webster TJ. Superparamagnetic Iron Oxide Nanoparticles (SPION) for the Treatment of Antibiotic-Resistant Biofilms. *Small.* 2012; 8(19): 3016–3027. <https://dx.doi.org/10.1002/smll.201200575>.
10. Shanan ZJ, Hadi SM, Shanshool SK. Structural Analysis of Chemical and Green Synthesis of CuO Nanoparticles and their Effect on Biofilm Formation. *Baghdad Sci J.* 2018; 15(2): 211-216. <https://dx.doi.org/10.21123/bsj.2018.15.2.0211>.
11. Ramasamy M, Lee J-H, Lee J. Potent antimicrobial and antibiofilm activities of bacteriogenically synthesized gold–silver nanoparticles against pathogenic bacteria and their physicochemical

- characterizations. *J Biomater Appl.* 2016; 31(3): 366–378. <https://dx.doi.org/10.1177/0885328216646910>.
12. Ali R, Shanan ZJ, Saleh GM, Abass Q. Green Synthesis and the Study of Some Physical Properties of MgO Nanoparticles and Their Antibacterial Activity. *Iraqi J Sci.* 2020; 61(2): 266-276. <https://dx.doi.org/10.24996/ijs.2020.61.2.9>.
13. Kote JR, Kadam AS, Ubaidullah M, Al-Enizi AM, Al-Abdrabnabi MA, Nafady A, et al. Antimycobacterial, Antioxidant and Cytotoxicity Activities of Mesoporous Nickel Oxide Nanoparticles for Healthcare. *Coatings.* 2020; 10(12): 1242. <https://doi.org/10.3390/coatings10121242>.
14. Al-Ogaidi I A. Detecting the antibacterial activity of green synthesized silver (Ag) nanoparticles functionalized with ampicillin (Amp). *Baghdad Sci J.* 2017; 14(1): 117-125. <https://dx.doi.org/10.21123/bsj.2017.14.1.0117>.
15. Khan S, Ansari AA, Khan AA, Abdulla M, Al-Obeed O, Ahmad R. In vitro evaluation of anticancer and biological activities of synthesized manganese oxide nanoparticles. *Med Chem Comm.* 2016; 7(8): 1647–1653. <https://dx.doi.org/10.1039/C6MD00219F>.
16. Varshni YP. Temperature dependence of the energy gap in semiconductors. *physica.* 1967; 34(1): 149-154. [https://dx.doi.org/10.1016/0031-8914\(67\)90062-6](https://dx.doi.org/10.1016/0031-8914(67)90062-6).
17. He Q, Liu J, Liu X, Li G, Chen D, Deng P. A promising sensing platform toward dopamine using MnO₂ nanowires/electro-reduced graphene oxide composites. *Electrochim Acta.* 2019; 296(10): 683–692. <https://dx.doi.org/10.1016/j.electacta.2018.11.096>.
18. He Q, Liu J, Liu X, Li G, Deng P, Liang J. Manganese dioxide Nanorods/ electrochemically reduced graphene oxide nanocomposites modified electrodes for cost-effective and ultrasensitive detection of Amaranth. *Colloids Surf B.* 2018; 172(1): 565–572. <https://dx.doi.org/10.1016/j.colsurfb.2018.09.005>.
19. Jayandran M, Haneefa MM, Balasubramanian V. Green synthesis and characterization of Manganese nanoparticles using natural plant extracts and its evaluation of antimicrobial activity. *J Appl Pharm Sci.* 2015; 5(12): 105-110. <https://dx.doi.org/10.7324/JAPS.2015.501218>.
20. Wan X, Yang S, Cai Z, He Q, Ye Y, Xia Y. Facile synthesis of MnO₂ nanoflowers/N-doped reduced graphene oxide composite and its application for simultaneous determination of dopamine and uric acid. *J Nanomater.* 2019; 9(6): 847. <https://dx.doi.org/10.3390/nano9060847>.
21. Holzwarth U, Gibson N. The Scherrer equation versus the 'Debye-Scherrer equation'. *Nat Nanotechnol.* 2011; 6: 534. <https://dx.doi.org/10.1038/nnano.2011.145>.
22. Ma C, Sun R, Chen Y, Sun J, Ji H, Li Y, et al. Freeze-drying preparation of MnOx/grapheme nanocomposite as anode material for highly reversible lithium storage. *J Mater Sci.* 2020; 55(13): 5545–5553. <https://dx.doi.org/10.1007/s10853-020-04395-y>.
23. Rahmat M, Bhatti HN, Rehman A, Chaudhry H, Yameen M, Iqbale M. Bionanocomposite of Au decorated MnO₂ via in situ green synthesis route and antimicrobial activity evaluation. *Arab J Chem.* 2021; 14(12): 103415. <https://dx.doi.org/10.1016/j.arabjc.2021.103415>.
24. Wilson DR, Green JJ. Nanoparticle Tracking Analysis for Determination of Hydrodynamic Diameter, Concentration, and Zeta-Potential of Polyplex Nanoparticles. *J Biomed Nanotech.* 2017; 15(7): 31-46. https://dx.doi.org/10.1007/978-1-4939-6840-4_3.
25. Manjula R, Thenmozhi M, Thilagavathi S, Srinivasan R, Kathirvel A. Green synthesis and characterization of manganese oxide nanoparticles from Gardenia resinifera leaves. *Mater Today: Proc.* 2020; 26(4): 3559–3563. <https://doi.org/10.1016/j.matpr.2019.07.396>.
26. Wang M, Meng Y, Zhu H, Hu Y, Xu C-P, Chao X, Li W, et al. Green Synthesized Gold Nanoparticles Using Viola betonicifolia Leaves Extract: Characterization, Antimicrobial, Antioxidant, and Cytobiocompatible Activities. *Int J Nanomedicine.* 2021; 16(9): 7319–7337. <https://dx.doi.org/10.2147/IJN.S323524>.
27. Muthukumar T, Sambandam B, Aravinthan A, Sastry TP, Kim JH. Green synthesis of gold nanoparticles and their enhanced synergistic antitumor activity using HepG₂ and MCF7 cells and its antibacterial effects. *Process Biochem.* 2016; 51(3): 384–391. <https://dx.doi.org/10.1016/j.procbio.2015.12.017>.
28. Boomi P, Ganesan RM, Poorani G, Gurumalles Prabu GH, Ravikumar S, Jeyakanthan J. Biological synergy of greener gold nanoparticles by using Coleus aromaticus leaf extract. *Mater Sci Eng C.* 2019; 99(25): 202–210. <https://dx.doi.org/10.1016/j.msec.2019.01.105>.
29. Du T, Chen S, Zhang J, Li T, Li P, Liu J. Antibacterial activity of manganese dioxide Nanosheets by ROS-mediated pathways and destroying membrane integrity. *J Nanomater.* 2020; 10(8): 1545. <https://dx.doi.org/10.3390/nano10081545>.
30. Huang J, Zhan G, Zheng B, Sun D, Lu F, Lin Y, et al. Biogenic silver nanoparticles by Cacumen Platycladi extract: synthesis, formation mechanism, and antibacterial activity. *Ind Eng Chem Res.* 2011; 50(15): 9095–9106. <https://dx.doi.org/10.1021/ie200858y>.
31. Khan SA, Shahid S, Lee C-S S. Green synthesis of gold and silver nanoparticles using leaf extract of Clerodendrum inerme; characterization, antimicrobial, and antioxidant activities.

Biomolecules. 2020; 10(6): 835.
<https://dx.doi.org/10.3390/biom10060835>.
32. Katoch M, Singh A, Singh G, Wazir P, Kumar R.
Phylogeny, antimicrobial, antioxidant and enzyme-

producing potential of fungal endophytes found in
Viola odorata. Ann Microbiol. 2017; 67(18): 529–
540. <https://dx.doi.org/10.1007/s13213-017-1283-1>.

التوليف الأخضر لجسيمات ثاني أكسيد المنغنيز النانوية وتقييمها البيولوجي

صبيحة خليل شنشول ، زينب جاسم شانان

قسم الفيزياء، كلية العلوم للبنات، جامعة بغداد، بغداد، العراق

الخلاصة

الهدف من هذا البحث هو تصنيع جسيمات نانوية لثاني أكسيد المنغنيز من المستخلصات النباتية (*A herba- P granatum L peel*، *C sinensis*، *M chamomilla L*، *alba Asso* and المستخلصات النباتية، تم استخدام تحليل مقياس الطيف الضوئي المرئي بالأشعة فوق البنفسجية (UV-Vis)، إمكانات زينا (ZP) و حيود الأشعة السينية (XRD). تبين أن تحضير جزيئات MnO_2 النانوية عن طريق المستخلصات النباتية له سمات مميزة. تم حساب متوسط الحجم البلوري لمركبات MnO_2 NPs المصنعة بين 14.22_21.0 نانومتر، مع قيم جهد زينا -23.6، -20.04، -25.6، -16.7 ملي فولت على التوالي. الجسيمات النانوية لثاني أكسيد المنغنيز (MnO_2 NPs) لها نشاط مضاد للجراثيم ضد الفطريات والبكتيريا المتنوعة الموجبة والسالبة لملون غرام. أظهرت النتائج أن MnO_2 NPs المحضر بواسطة *A Asso*، *P granatum L peel* *herba-alba* كان أعلى نسبة من تثبيط البكتيريا و الفطريات، بينما أظهرت مستخلصات *chamomilla L M* و *C sinensis* نشاطاً مضاداً أقل.

الكلمات المفتاحية: مضادات الميكروبات، الفطريات، ثاني أكسيد المنغنيز MnO_2 ، قشر الرمان، جهد زينا.